DOI: https://doi.org/10.14256/JCE.3305.2021

Građevinar 6/2023

Primljen / Received: 11.7.2021.
Ispravljen / Corrected: 27.8.2022.
Prihvaćen / Accepted: 6.1.2023.
Dostupno online / Available online: 10.7.2023.

Investigation of the use of waste mineral additives in ultra-high-performance concrete

Authors:

Assoc.Prof. **Selçuk Memiş**, PhD. CE
Kastamonu University, Turkey
Department of Civil Engineering
smemis@kastamonu.edu.tr
Corresponding author

Ali Alshaab Ramroom , MCE
Kastamonu University, Turkey
Department of Civil Engineering
ali.ramrom@gmail.com

Research Paper

Selçuk Memiş, Ali Alshaab Ramroom

Investigation of the use of waste mineral additives in ultra-high-performance concrete

This study examined the effects of various waste materials on the properties of ultra-high-performance concrete (UHPC), along with their designs and ideal mix ratios. Several UHPC mixtures have been developed using the Taguchi L16 method, which generally forms part of the experimental programs for evaluating the properties of UHPCs. Furthermore, the proportions of the component materials were chosen based on approximate ranges found in literature. The samples were cured under two different regimes: standard immersion water curing (SC) and hot water immersion curing (HC). The properties of both hardened and fresh concretes were assessed. A flow test was conducted on the fresh concrete to determine the workability, and a standard test was conducted to assess the density. To investigate a hardened concrete sample, the compressive and flexural strengths were examined and density, absorption, and void tests were conducted. The results obtained from the Taguchi approach for the compressive strength at 28 days were found to be 20 % for SF, 0 % for FA, and 0 % for GBFS; the flexural strength was 10 % for SF, 0 % for FA, and 0 % for GBFS. The compressive strength was 147.07 MPa with SC and 150.13 MPa with HC and flexural strength was 26.88 MPa with SC and 27.31 MPa with HC (as conducted at 28 days in a mixture of 10 % SF and 10 % GBFS).

Key words:

ultra-high-performance concrete (UHPC), cement, steel fibre, polycarboxylate ether-based superplasticizers (PCEs), compressive strength

Prethodno priopćenje

Selçuk Memiş, Ali Alshaab Ramroom

Ispitivanje primjene otpadnih mineralnih dodataka u betonu ultravisokih svojstava

Ovo istraživanje ispituje utjecaj različitog otpadnog materijala na svojstva betona ultravisokih svojstava (UHPC), kao i način njihova projektiranja i idealne omjere mješavine. Primjenom metode Taguchi L16 razvilo se nekoliko UHPC mješavina, a što općenito oblikuje eksperimentalne programe za procjenu svojstava UHPCA-a. Nadalje, izabrani su omjeri sastavnih materijala na temelju približnih dosega nađenih u literaturi. Uzorci su njegovani na dva različita načina, a to su: standardno njegovanje uranjanjem u vodu (SC) i njegovanje uranjanjem u vruću vodu (HC). Primijenjena su svojstva očvrsnulog i svježeg betona. Provedeno je ispitivanje betona u svježem stanju kako bi se odredila obradivost te se provelo standardno ispitivanje gustoće. Kako bi se ispitao očvrsnuli uzorak betona, proučene su tlačna čvrstoća i čvrstoća pri savijanju, a provedena su ispitivanja gustoće, apsorpcije i poroznosti. Rezultati tlačnih čvrstoća nakon 28 dana dobiveni Taguchijevim pristupom iznosili su 20 % u slučaju SF-a, 0 % u slučaju FA-a i 0 % u slučaju GBFS-a, a čvrstoće pri savijanju iznosile su 10 % za SF, 0 % za FA i 0 % za GBFS. Tlačna je čvrstoća bila 147.07 MPa u slučaju SC-a, 150.13 MPa u slučaju HC-a, a čvrstoća pri savijanju bila je 26.88 MPa u slučaju SC-a i 27.31 MPa u slučaju HC-a (jer se provodi nakon 28 dana u mješavini s 10 % SF i 10 % GBFS).

Ključne riječi:
beton ultravisokih svojstava (UHPC), cement, čelična vlakna, superplastifikatori na bazi polikarboksilatnog etera (PCE), tlačna čvrstoća

1. Introduction

Concrete is an extensively used building material owing to its good strength and durability. It is the most common man-made building material and has the necessary mechanical and durability properties to be made into the desired shapes and sizes; it is also a relatively low-cost material [1–10]. Certain advanced civil engineering design facilities (such as high-rise buildings and nuclear power plants) constructed using ultra-high-performance concrete (UHPC) have been specifically designed considering extreme loading in adverse events, such as a missile attack or an aircraft impact, owing to the dire consequences if such structures were to fail [11].

UHPC is a desirable material for these types of structures. Recently, UHPC has been extensively studied as it can improve the lifespans and economic efficiency of structures. The deterioration of civil infrastructure has drawn worldwide attention owing to the large amounts of annual outlays required for repair and rehabilitation, as well as the profound detrimental impacts on society and the environment [11, 12]. Thus, sustainable construction materials have attracted considerable research interest, including concretes with reduced embodied energies, reduced carbon footprints and enhanced durability [13, 14]. Ecological goals such as reducing non-renewable resource extraction, regenerating renewable energy and reducing residues and wastes require using improved building materials. The appropriate usage of raw materials is essential for building material production; moreover, it is necessary to recycle wastes in a way that meets future requirements [6–9, 14]. In addition, the innovative materials and methodologies being developed will likely extend the infrastructural lifetime. Experts are interested in UHPC because, a novel cementing material, it can provide improved infrastructural durability and increase the service lives of buildings [15, 16]. First introduced in France during the 1990s, UHPC exhibits higher strength than conventional high-strength concretes [17, 18]. Replacing conventional concretes with UHPCs allows for the development of smaller structural components/members. The construction of smaller members is associated with reductions in transportation, formwork, labour and maintenance costs. The high strength of UHPC also assures its sustainability through the construction of slim and durable designs. A UHPC's high durability mainly arises from its resistance against all types of corrosion; this increases the design life of a project and reduces the maintenance costs [11, 19]. For instance, UHPC has extremely low permeability against chloride penetration (one of the factors with the strongest effects on improving durability). Other properties of UHPC facilitating its high durability include its lower total porosity, micro-porosity, water absorption and chloride ion diffusion [19, 20].

Alsalman et al. (2020) developed several UHPC blends using locally available materials and investigated the effects of the binder content high-range water reducer admixture, steel fibre, mixer and curing regime on the compressive strength [21]. Meng et al. (2016) developed systematic mixture designs using mathematical models and used fly ash (FA), silica fume (SF) and granulated blast furnace slag (GBFS) to obtain UHPC at a relatively low cost. They used traditional concrete sand and relatively low fibre content and proposed several cost-effective UHPC blends with various ingredients. They then evaluated the basic processability, strength and durability these blends [12]. Hou et al. (2021) investigated the use of red sludge obtained from landfills with SiO_2 (equivalent to cement) as a mineral additive in the development of UHPCs, together with SF and FA [18]. In general, SF fills the voids in the paste matrix, accelerating the pozzolanic reactions that generate additional calcium silicate hydrates. In addition, it is 4–7 times cheaper than cement. The use of an optimised SF as well as FA and GBFS reduces the UHPC costs without affecting the concrete properties [12]. Hung et al. (2020) examined the processability and fibre distributions of hooked-end steel macro-fibre-reinforced UHPCs with various fine aggregates and fibre contents. They investigated the effects of various variables on the mechanical properties of this type of UHPC on the 28th and 90th days [22]. Memiș and Ramrom (2020) studied the effects of the ideal ratio of mineral additives as specified in references on UHPC production and the effects of the ideal steel fibre ratio on concrete [23]. Shen et al. (2020) investigated the effects of incineration bottom ash on a UHPC's mechanical properties, workability, hydration, volume stability and microstructure by reusing the base ash from an urban solid waste incinerator as a fine aggregate to prepare a UHPC with SF and FA additives [24].

This study investigated the economic production of SF, FA and GBFS from industrial wastes for providing the necessary high strength to UHPCs (in addition to the properties of normal concretes). The Taguchi L16 matrix was used to examine the efficiency of the UHPC production.

2. Material and methods

2.1. Materials

The UHPC production process used included washing silica sand from an 0–2 mm sieve obtained from the city of Kastamonu, Turkey. The particle size distribution of the sand used in the study is shown in Table 1. In addition, the process used Type 1 Portland cement (PC; CEM II / A-M (P-L) 42,5R). The PC was a general use cement (Portland composite cement) created according to TS EN 197-1 standard [25]. The cement's specific weight was 2.94 g/cm^3 and the Blaine surface area was 4191 cm^2/g. The SF used in the concrete production was obtained from the Antalya Etimine Electro-Ferrochrome Plant and used according to the American Society for Testing and Materials (ASTM) C 1240 standard [26]. The specific gravity of the SF was 2.19 and the Blaine surface area was 23.36 m^2/g. The other pozzolanic materials used in the cement were FA and GBFS. The FA was used as a mineral admixture and was classified according to TS EN 197-1 as V-type [25]; it was also classified as F-type according to ASTM C 618 [27]. The GBFS was provided by the Ereğli Iron & Steel Works Company in Kdz. Ereğli, Turkey.

Table 1. Sieve analysis of silica sand used in the study [28]

Sieve	Weight [g]	Remaining in the sieve [%]	Percentage passing [%]	ASTMC33 [%]
9.5 mm	0	0	100	100
4.75 mm	0	0	100	95 – 100
2.36 mm	0	0	100	80 – 100
1.18 mm	35.61	7.12	92.88	50 – 85
600 μm	138.7	34.86	65.14	25 – 60
300 μm	187.42	72.35	27.65	5 – 30
150 μm	102.47	92.84	7.16	0 – 10
Pan	35.80	100	0	
Fineness module according to ASTM C 136 (2014.) = 2.14 [29]				

Table 2. Chemical compositions and physical and mechanical properties of materials

Chemical composition [%]	Portland cement (PC)	Fly ash (FA)	Silica fume (SF)	Granulated blast furnace slag (GBFS)
CaO	63.59	1.77	0.44	37.79
SiO_2	20.90	61.81	80.9	35.09
Al_2O_3	5.53	9.54	0.34	17.54
Fe_2O_3	3.70	7.01	0.55	
MgO	1.76	2.56	5.23	5.75
Na_2O	0.18	2.43	0.35	0.74
K_2O	0.41	0.99	4.5	0.28
SO_3	0.73	0.31	-	0.19
Cl	0.0027	-	0.13	
Free CaO	2.56	-	2.70	
Physical and mechanical properties of cement				
Compressive strength, 2 days [MPa]	17.9			
Compressive strength, 7 days [MPa]	31.7			
Compressive strength, 28 days [MPa]	45.9			
Specific gravity	2.94	2.76	2.19	2.95
Initial setting time [min.]	177			
Final setting time [min.]	233			
Volume stability [cm²/g]	1			
Blaine value [cm²/g]	4191	3300	2390	3500
90 μm passing [%]	98.8			
32 μm passing [%]	88.5			

The chemical compositions of the GBFS and FA are shown in Table 2. The PC conforming to the TS EN 197-1 [25] standard requirements was obtained from the Bolu Cement Industry Inc., Turkey. Detailed information regarding the physical and chemical properties of the cement used in this experiment is shown in Table 2.

This study used steel fibre with a diameter of 0.15 mm, length of 13 mm, specific gravity of 7.8, tensile strength of 3000 MPa and modulus of elasticity of 200 GPa. Polycarboxylate ether-based superplasticizers (PCEs) were adsorbed electrostatically on the cement surface with negatively charged carboxylic acids on the polymer surface. Owing to this absorption, polyethylene glycol side chains [30] could be used as the superplasticizers in this study because they were stretched towards the water phase, thereby providing a good cement-dispersing effect.

2.2. Mix design and specimen preparation

The design of the mixture was determined using the Taguchi L16 matrix [31-34]. A naming system was developed to understand and indicate the compositions of these different mixtures. Each mixture was given a code (Table 3) with a specific letter identifier. In particular, "S" was used for SF, "F" for FA and "G" for GBFS. In addition, group codes were created by writing the percentage used after each letter. For example, S15F20G10 denoted a UHPC mixture containing 15 % SF, 20 % FA and 10 % GBFS.

Table 3. Considered levels for each parameter in Taguchi L16 matrix design of experiment

Parameters	Code	Level [%]			
			2	3	4
SF	S	0	10	15	20
FA	F	0	10	15	20
GBFS	G	0	10	15	20

Table 4. L16 array as suggested by Taguchi for three parameters at four levels

	Mixture	Parameters		
		SF	FA	GBFS
1	Reference	0	0	0
2	S0F10G10	0	10	10
3	S0F15G15	0	15	15
4	S0F20G20	0	20	20
5	S10F0G10	10	0	10
6	S10F10G0	10	10	0
7	S10F15G20	10	15	20
8	S10F20G15	10	20	15
9	S15F0G15	15	0	15
10	S15F10G20	15	10	20
11	S15F15G0	15	15	0
12	S15F20G10	15	20	10
13	S20F0G20	20	0	20
14	S20F10G15	20	10	15
15	S20F15G10	20	15	10
16	S20F20G0	20	20	0

A total of 16 groups of mixtures were prepared using the Taguchi L16 matrix (Table 4). As shown in Table 4, the matrix comprised an L16 orthogonal array (three parameters at four levels) showing all factors and levels [32–34]. The quantities of the materials used in these mixtures are provided in Table 5.

In all of the UHPCs produced in this study, the pretesting mixtures and cement dosages as determined by the literature (Table 6) were kept constant; for example, the binder weight remained at 1000 kg/m³. In addition, the water/binder ratio (w/b) was 0.19 and the PCE/binder ratio was 3.5 %. While the blends had a sand/binder ratio of 1:1 (by weight), the amounts of steel fibre were kept constant at 1 % by volume in the same volume. The w/b was adjusted to 0.2 for the control mixture only. The effects of the sand and reinforcing fibres on the properties of the mixtures were examined in the context of choosing the best ratio for the study. In the mixtures prepared for this purpose, the sand, SF, GBFS and FA were kept at 105 °C for 24 h so that the materials were freed from moisture and could be used in dry mixes. The mixtures were specially prepared as UHPC mixtures. For this purpose, the mixing process for UHPC mixtures, as specified in Torregrosa (2013) was followed (Table 7) [35] for the UHPC production. The materials were mixed using a Hobart-type mixer (LTC 320 model) with 1100-W power and a 10-L boiler. Each mixed material was set aside after the procedure.

The mixes prepared in the concrete mixer were moved sideways with the bucket to align the fibres for as long as possible and then were poured into prismatic moulds of 4 × 4 × 16 cm³.

In general, temperature and humidity are important factors in improving the mechanical properties of UHPCs. For example, the properties of UHPCs can be improved by using heat-curing regimes to accelerate the early strength of the concrete [21, 44]. In this study, the UHPC samples were removed from the moulds

Table 5. Mixture proportioning [kg/m³] and fresh properties for ultra-high-performance concrete (UHPC)

Mixture	Cement	SF	FA	GBFS	Sand	Steel fibre	Water	PE	Slump [cm]		Fresh unit weight [kg/m³]
									Static	Dynamic	
Reference	1000	0	0	0	1000	78	190	35	200	240	2345
S0F10G10	800		100	100					210	250	2352
S0F15G15	700		150	150					240	270	2310
S0F20G20	600		200	200					250	280	2354
S10F0G10	800	100	0	100					210	240	2350
S10F10G0	800		100	0					200	230	2310
S10F15G20	550		150	200					250	270	2314
S10F20G15	550		200	150					250	280	2346
S15F0G15	700	150	0	150					200	230	2356
S15F10G20	550		100	200					200	220	2340
S15F15G0	700		150	0					210	230	2320
S15F20G10	550		200	100					240	260	2310
S20F0G20	600	200	0	200					190	220	2358
S20F10G15	550		100	150					200	230	2312
S20F15G10	550		150	100					190	220	2335
S20F20G0	600		200	0					190	220	2313

Table 6. Use of studies to determine ideal ratios

Selected ratio [%]	Selected ratio
Binder weight = 1000 kg/m^3	[15, 23, 35–38]
Water-to-binder ratio (w/b) = 0,20	[15, 23, 39, 40]
Polycarboxylate ether-based superplasticizer (PCE)-to-binder ratio = 3.5 %	[23, 35, 41]
SF-to-binder ratio = 20 %	[23, 36, 39, 42]
Steel fibre to volume = (0, 0.5, 1.0, 2.0) %	[15, 43]

Table 7. Mixing process of the study

Min	Process	Aspect	
0 – 1	Sand and binder mixing	Dry	
1 – 3	Adding water and 50 % PCE	Dry - plastic	
3 – 4	Stop the mixer	Plastic	
4 – 6	Mixing after adding the left over PCE	Plastic - fluid	
6 – 7	High-speed mixing	Fluid	
7 – 10	Mixing after adding steel fibre	Fluid	

24 h after the casting process was completed. Subsequently, they were then cured using standard water curing (SC) as per ASTM C192 until the day of the experiment [45] and using hot water immersion curing (HC) (24 h in 65 °C hot water and 23.0 + 2.0 °C water) until the day of the experiment.

2.3. Test procedures

An important feature of a UHPC is its self-levelling ability. To test this feature, the modified ASTM C1437 [46] standard was used to ensure a hydraulic UHPC mortar flow. The spreading diameter (Figure 1) was measured after the material was allowed to stabilise in all directions; this method measures the actual diameter (mm) of the material before compression (static flow) and spread diameter (dynamic flow) as a result of compression after 25 drops. In addition, the fresh-state UHPC density was determined according to the ASTM C 138 [47] standard and was calculated by dividing the weight of the material placed into the mixture by the volume occupied (T = M/V).

Compressive and flexural strength tests are among the tests for hardened-state properties; in this study, they were conducted on samples after completing their 3rd, 7th and 28th days of curing. These tests were conducted in an experimental process according to the BS EN 196-1 [48] standard. Specifically, 40 × 40 × 160 mm samples were placed horizontally on two supports spaced 100 mm apart. To test the flexural strength, a vertical load was applied with a loading cylinder on the upper surface of the prism at a rate of 50 ± 10 N/s^1 until breakage occurred. The compressive strength tests of the UHPC samples were performed on two parts obtained from the flexural strength tests. For this purpose, the UTEST LC815 brand cement tester (maximum capacity of 250,000 lb) was used. Using the obtained force (Fr), the flexural strength was calculated with the equation Rf = (1.5 Fr L)/b^3.

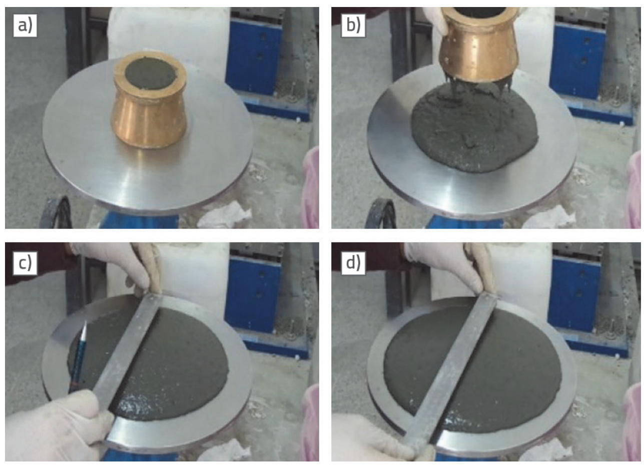

Figure 1. Flow test setups and spread measurements: a) Konus ispunjen materijalom; a) The cone filled with material; b) The cone is removed and mix spread; c) Static flow; d) Dynamic flow (after 25 drops)

In the compressive strength test, a loading speed of 2400 ± 200 N/s^1 was applied to each one of the pieces as broken in response to the flexural strength at the device jaw with a size of 40 × 40 mm. Thus, the compressive strength value was calculated with the help of the sample-breaking load. In addition, the absorption, density and void ratio were determined according to ASTM C642 [49]. This standard can also be useful for developing conversion data for concrete masses and volumes;

correspondingly, it can help determine the concrete specifications and identify differences or variations in different locations.

3. Results and discussion

3.1. Fresh properties

The results from the flow test for measuring workability are shown in Table 5. The actual diameter of the material was measured in mm in both pre-tamping (static flow (Figure 1.c)) and post-tamping (dynamic flow (Figure 1.d.). Generally, pozzolanic admixtures such as SF, GBFS and FA may provide an excellent workability effect to UHPCs. Notably, the flows of the mixes of UHPCs with high pozzolanic additives were highly fluid. Figure 2.a shows the relationship between the SF content and dynamic flow. Previous studies demonstrated that using SF as a filler causes a decrease in the dynamic flow rate. The effect of SF on the workability of a UHPC is relatively complicated. In previous studies, some researchers found that SF could improve the workability of a UHPC [50, 51]. However, other researchers concluded that SF decreased the workability of a UHPC [52, 53].

As shown in Figure 2, an increase in the ratio of FA and GBFS leads to an improvement in the dynamic machinability of the UHPC mixture. Conversely, an increase in silica fume (SF) ratio leads to a decrease in machinability. The effect of the dynamic flow on the machinability is similar to that described by Bajaber and Hakeem (2021), i.e., FA and GBFS positively affect the increase in machinability [53]. The different conclusions may be attributed to the different characteristics of the raw materials and the effect of superplasticizer in SF. It is likely that the use of superplasticizer in SF, with its small particle size, high specific surface area and high water demand, reduces the fluidity of the UHPC mixture. When mixed with superplasticizer, the fine and round particles of SF are covered by a layer of the surface-active compound, resulting in a repulsive electric force between the particles of cement and additive. As the SF particles are much smaller than those of cement, they act as ball-bearings between the cement particles, increasing the fluidity of the cement paste, [54]. Figures 2.b and 2.c show the improvements in the flow of UHPC mixtures for FA and GBFS. As the content of these materials in the mixtures increases from 0 % to 20 %, the flow of the mixture also increases (Figure 2.d). The spherical shape of FA particles helps to reduce the water requirement, resulting in high levels of workability. Additionally, the spherical shape reduces the friction between sand particles, leading to better lubrication and

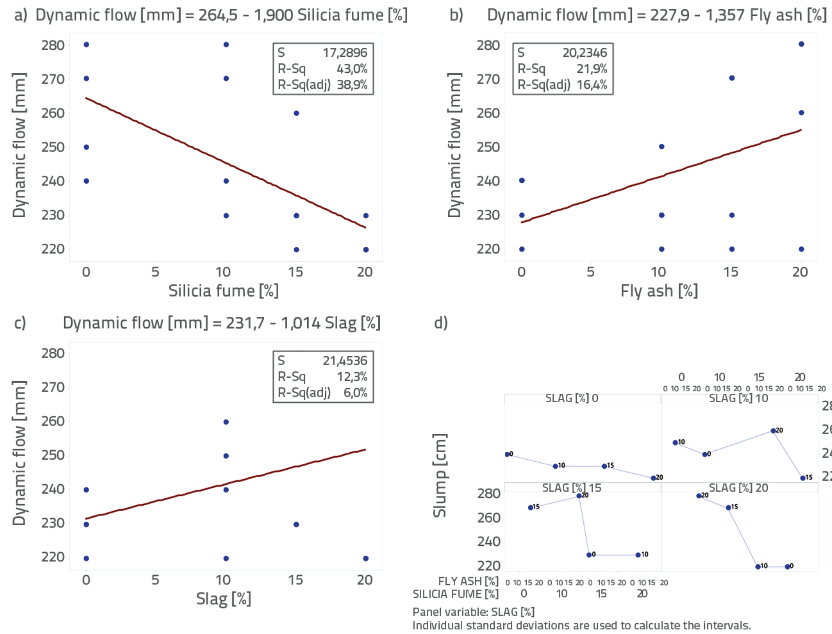

Figure 2. Relationship between dynamic flow and mineral content

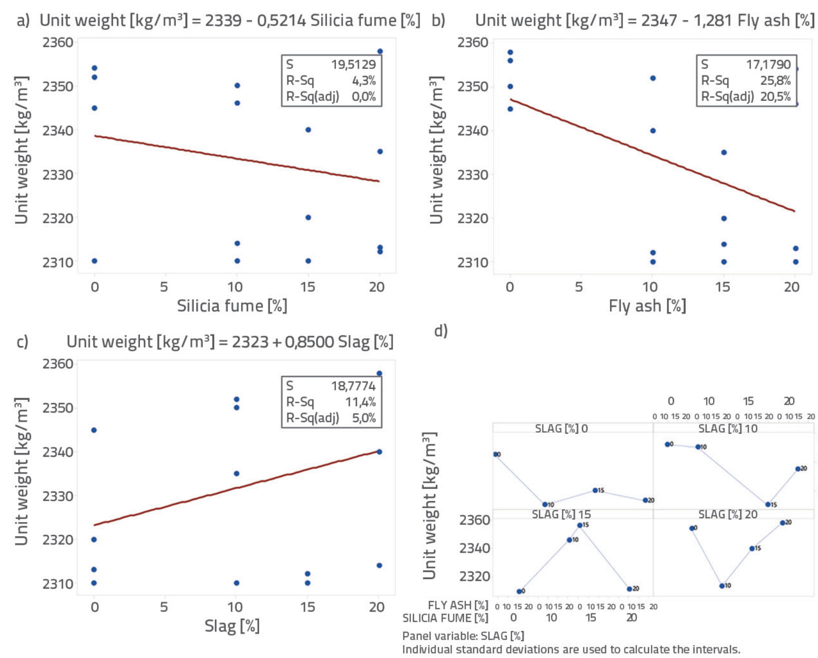

Figure 3. Relationship between fresh unit weight and mineral content: a) Unit weight- SF; b) Unit weight – FA; c) Unit weight – GBFS; d) Effect of additives on unit weight

improved flow of the concrete. The greater the percentage of FA in the concrete paste, the better the lubrication of particles and the better the flow of the concrete [55].

The test results for the unit weight of fresh concrete are shown in Table 5. The unit weight ranges from 2310 to 2356 kg/m^3. Adding SF and FA to the UHPC mixtures decreases the fresh unit weight as shown in Figure 3, whereas adding GBFS increases the unit weight (Figure 3.c). This is because the specific gravities of the pozzolanic mineral admixtures (2.26 kg/m^3 for SF, 2.75 kg/m^3 for FA and 2.95 kg/m^3 for GBFS) are less than the specific gravity of the cement (3.15 kg/m^3); thus, the admixture volume is larger than that of the paste from the substituted cement [54].

3.2. Hardened properties

3.2.1. Results of compressive strength tests

Compressive strength tests were conducted on the 3th, 7th and 28th days of SC and on the 28th day of HC in accordance with BS EN 196-1 [48], as shown in Table 8. The compressive strength on the 28th day in the HC was significantly higher than in all SC periods. The highest percentage increase was 21 % in mixture group S15F10G20 and the lowest percentage increase was 0.9 % in the control mixture. This can be attributed to the effect of the accelerated hydration on the compressive strength in the concrete owing to the greater heat relative to SC. Moreover, the pozzolanic reactions are also accelerated by the higher curing temperatures. As is well-known from the literature, the temperature of the curing regime plays a vital role in increasing the strength (Figure 4.a). Owing to the high percentage of cement in a UHPC, a hot environment leads to the rapid hydration of cement; this results in high proportions of hydrated products, which in turn leads to high strength [56].

The compressive strength test results show compressive strengths of 147.07 MPa under SC and 150.13 MPa under HC. The temperature change according to the statistical averages is given in Figure 4.

The use of FA and GBFS at a content-to-binder percentage between 20 %–35 % decreases the compressive strength of the UHPCs at early ages. However, SF significantly improves the compressive strength. A comparison of the 28-day compressive strengths reveals that adding 10 % SF and 10 % GBFS improves the compressive strength by 24 % relative to the control. As shown in Figure 5, the effect of the addition of SF can be assessed by comparing the compressive strengths at 28 days. In SC, the strength is increased when the quantity of SF is increased. A similar phenomenon has been observed and attributed to the filler and pozzolanic effects of SF [50, 51].

As shown in Figure 5b and Figure 5c, the compressive strength in SC decreases at 28 days with increased quantities of FA and GBFS. This phenomenon may be attributed to the use of FA, which leads to a decrease in strength in the early age of concrete at up to 28 days [55]. Maltais and Marchand (1997) reported that when curing at 20 °C, depending on the cement replacement level and type of FA, the compressive strengths of

Table 8. Compressive strength and flexural strength test results for mixtures

Mix No.	Mix code	Compressive strength [MPa]				Flexural strength [MPa]			
		3 days (SC)	7 days (SC)	28 days (SC)	28 days (HC)	3 days (SC)	7 days (SC)	28 days (SC)	28 days (HC)
1	Reference	97.62	109.69	118.35	119.13	14.65	21.27	22.66	23.05
2	S0F10G10	74.85	92.60	94.28	110.05	15.38	18.33	22.03	22.59
3	S0F15G15	66.55	88.59	106.84	115.84	12.61	20.70	22.08	22.84
4	S0F20G20	64.16	79.25	106.21	114.25	13.53	16.48	21.94	22.05
5	S10F0G10	93.36	114.66	147.07	150.13	16.46	18.19	26.88	27.26
6	S10F10G0	87.85	112.74	139.32	146.05	16.29	22.99	26.27	27.31
7	S10F15G20	71.24	92.70	127.43	137.88	11.11	16.39	18.28	19.92
8	S10F20G15	72.63	94.12	121.83	142.70	10.78	14.79	18.31	21.00
9	S15F0G15	95.39	117.66	139.35	144.04	15.63	18.96	23.25	24.18
10	S15F10G20	68.81	91.09	115.05	139.78	14.46	15.64	19.48	21.34
11	S15F15G0	86.9	109.63	131.46	144.74	15.29	16.31	22.76	22.97
12	S15F20G10	72.58	89.71	123.17	140.07	12.42	13.55	15.89	18.30
13	S20F0G20	81.25	110.04	139.48	147.36	14.95	19.32	22.64	22.98
14	S20F10G15	75.65	100.48	130.91	133.87	13.69	18.21	21.75	23.23
15	S20F15G10	74.07	99.47	138.34	140.83	17.53	17.95	21.12	23.78
16	S20F20G0	81.9	110.17	133.50	135.51	16.55	17.21	22.52	23.33

(SC) Standard curing,. (HC) Hot water curing

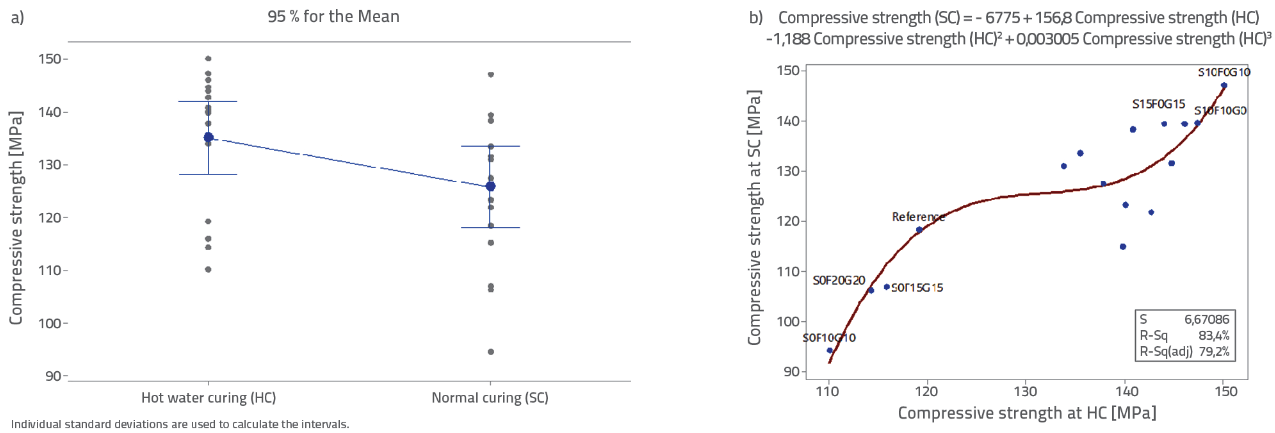

Figure 4. Compressive strength range distribution at every stage of testing

FA mortars can take from 25 to 50 days to reach that of a reference mixture [57]. Generally, the pozzolanic reactions of FA in cement systems under SC become dominant after 28 days [58]. According to Wang et al. (2004), the activity of FA is not completed until 365, with only 36.56 % of it reacting [59]. This depends on two important factors: the activity of FA by itself and the role of FA in promoting the hydration of the cement. It is uncertain whether the pozzolanic reaction will continue to occur for all of the active FA in the system; this depends on the $Ca(OH)_2$ (promoted by the cement hydration) and is important for continuing the pozzolanic activity. An increase in FA content leads to a decrease in the total hydration of the system as the activity of FA is lower than that of cement.

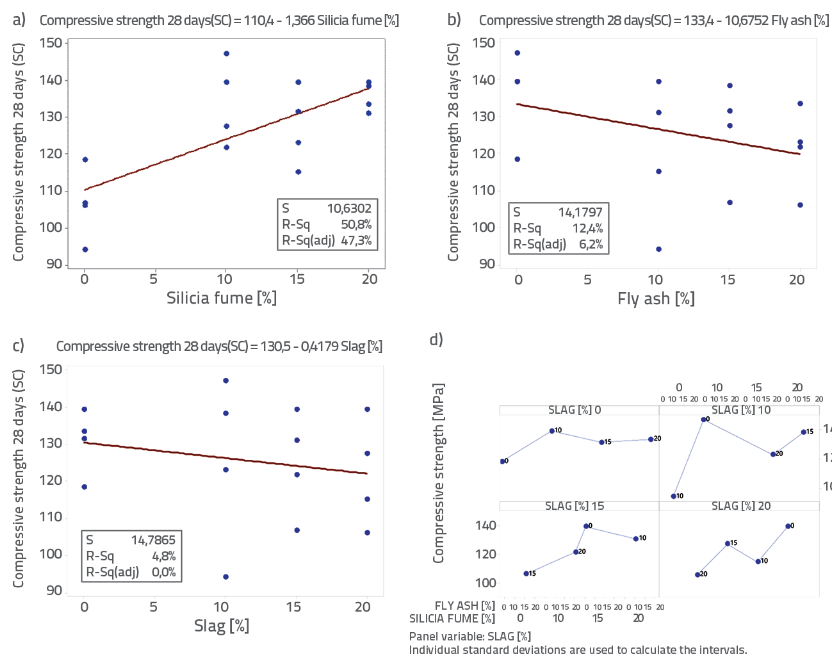

Figure 5. Mineral admixtures impact on compressive strength results

3.2.2. Results of flexural strength tests

The flexural strengths of UHPCs after different curing conditions (SC and HC) on the 3rd, 7th and 28th days are presented in Table 8 in accordance with BS EN 196-1 [48]. The results indicate that the highest flexural strength was observed in the S10F0G10 mixture, with a value of 26.88 MPa at 28 days of curing under SC conditions, representing an approximate 118 % increase in strength compared to the reference mix. The lowest flexural strength was observed in the S15F20G10 mixture, with a value of 15.89 MPa, which was less than that of the reference mix, as depicted in Figure 6. Furthermore, the flexural strength of each group increases with the progression of time in HC, regardless of the type of concrete. This improvement is especially evident from the 7th to 28th day.

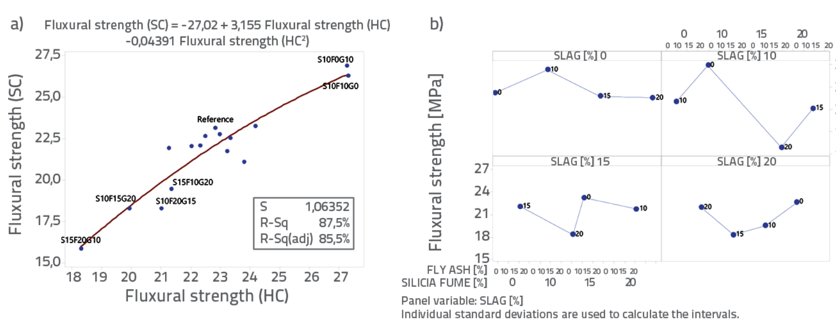

Figure 6. Flexural strength range distribution at every stage of testing

Table 9. Results for water absorption rate, porosity, and apparent density

Mix code	Absorption after immersion [%]	Absorption after immersion and boiling [%]	Volume of permeable voids [%]	Bulk density, dry [kg/m³]	Bulk density after immersion [kg/m³]	Bulk density after immersion and boiling [kg/m³]	Apparent density [kg/m³]
Reference	3.10	1.10	2.49	2335	2407	2351	2374
S0F10G10	2.49	0.96	2.25	2342	2400	2364	2396
S0F15G15	2.44	1.05	2.47	2351	2408	2376	2410
S0F20G20	2.06	0.72	1.68	2344	2393	2361	2385
S10F0G10	1.22	0.59	1.41	2388	2417	2402	2422
S10F10G0	1.30	0.68	1.60	2357	2387	2373	2395
S10F15G20	1.45	0.59	1.41	2389	2424	2403	2423
S10F20G15	1.29	0.65	1.54	2383	2413	2398	2420
S15F0G15	1.38	0.65	1.55	2385	2418	2401	2423
S15F10G20	1.23	0.57	1.34	2356	2385	2370	2388
S15F15G0	1.16	0.56	1.31	2362	2389	2375	2393
S15F20G10	1.00	0.42	0.99	2368	2392	2378	2392
S20F0G20	1.29	0.71	1.67	2354	2384	2371	2394
S20F10G15	1.29	0.73	1.72	2342	2372	2359	2383
S20F15G10	1.26	0.70	1.64	2330	2359	2346	2369
S20F20G0	1.19	0.66	1.53	2326	2353	2341	2362

3.2.3. Determination of density, absorption and voids

The test results for the density, percentage absorption and percentage of voids in the hardened concrete according to ASTM C642 [49] are shown in Table 9. Table 9 shows that the water absorption and voids of UHPCs with SF, FA and GBFS decrease relative to those of control mixture. The decrease in water absorption could result from the pozzolanic reactions reducing the sizes of the pores of the concrete.

By examining the effects of the SF, FA and GBFS on the water absorption rate, porosity and apparent density (Figure 7), it can be seen that SF is more effective in UHPCs than the other additives. In addition, depending on the ratio of its increase, it can cause decreases in the water absorption rate (Figure 7.a) and porosity (Figure 7.b). This could be owing to the very fine particles of the SF filling the pores in the concrete. In addition, Figure 7.a, 7.d, 7.g and 7.j show the relationship between the water absorption and percentage of FA in the mixtures; the water absorption changes by approximately 1.0 % to 1.8 %. The porosity (Figure 7b, Figure 7h, Figure 7k) causes a change of approximately 1.4 % to 1.8 % depending on the ratio of increase of the SF, FA and GBFS. These data demonstrate that the water absorption and porosity of the UHPC decrease with an increasing concentration of the microparticles in the composite material, owing to the reduced proportion of open pores in the rigid UHPC. An open-cell contains air and is the same size as the microparticles (filler particles). Therefore, as the water absorption depends on the number of communicating openly connected cells, filling the open pores with microparticles reduces the water absorption.

However, an increase in the GBFS content results in a slight increase in the apparent density (Figure 7i). Insofar as similar changes in the apparent density based on the additive (Figure 7c, Figure 7f, Figure 7i, Figure 7l), increasing the SA, FA and GBFS ratios results in a change between 2360 and 2425 kg/m^3 (depending on the ratios). Adding SF and FA in UHPC mixtures leads to a decrease in dry-bulk density, whereas adding GBFS increases it. This can be attributed to the fact that the specific gravity of the pozzolanic mineral admixtures is lower than that of the cement [54]. These results are consistent with those of Sunil et al. (2015), who found that density decreased with an increasing amount of FA, as the specific gravity of FA is lower than that of cement [60].

3.3. Taguchi optimisation

3.3.1. Taguchi analysis for strengths

To determine the ideal mixture based on the results obtained by using the Taguchi L16 test matrix, the optimum results for the compressive and flexural strengths according to the effects of the curing conditions are shown in Figure 8. The optimum levels of these results are listed in Table 10.

As a result of the optimisation analysis, it was determined that one group in L16 mixture was the same mixture and was not absent in this mixture in two different mixtures. The ideal optimum result for the compressive strength is when using the S20F0G0 mixture, i.e., 20 % SF, 0 % FA and 0 % GBFS under SC conditions. In contrast, under HC conditions, the

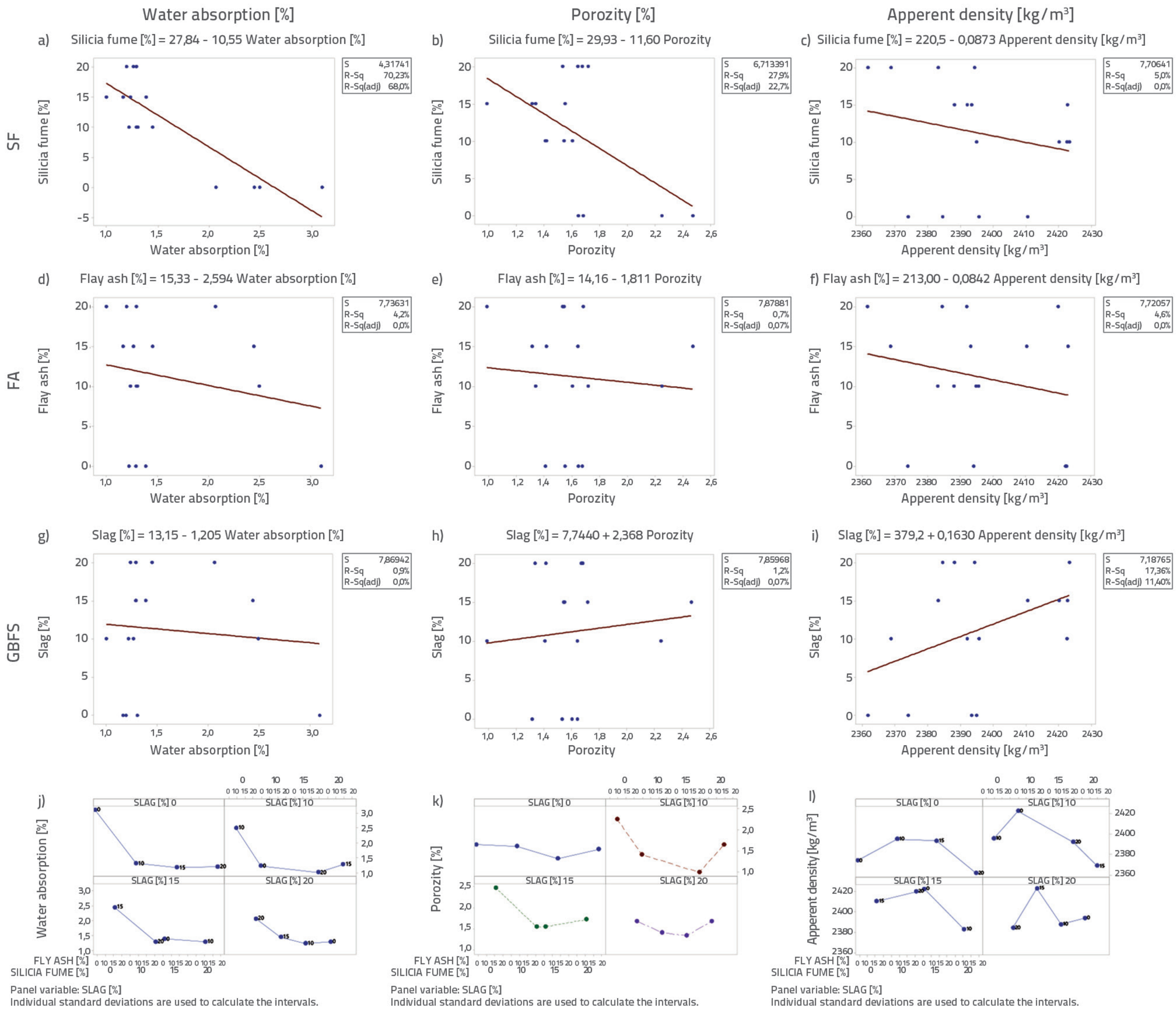

Figure 7. Effect of mineral additives on water absorption rate, porosity, and apparent density

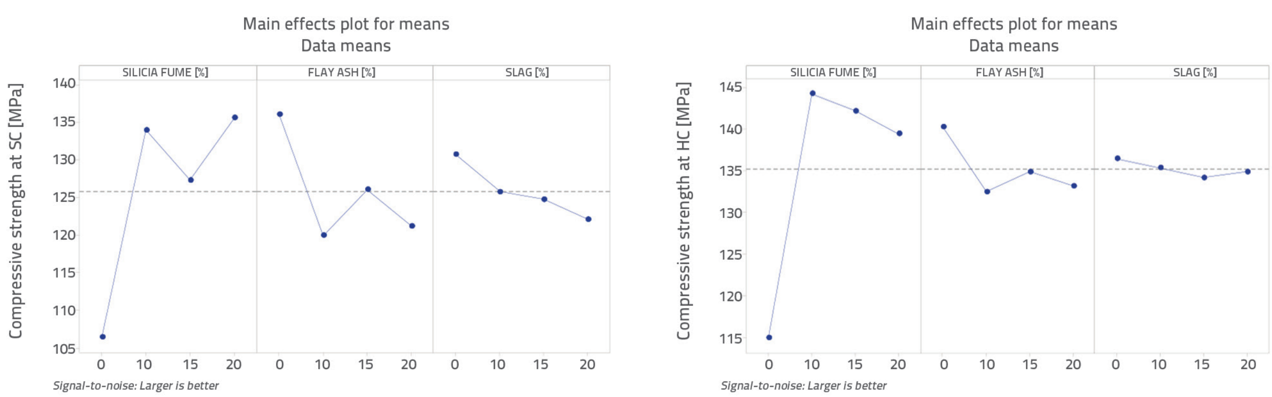

Figure 8. Taguchi optimisation control factor graphs - 1st part

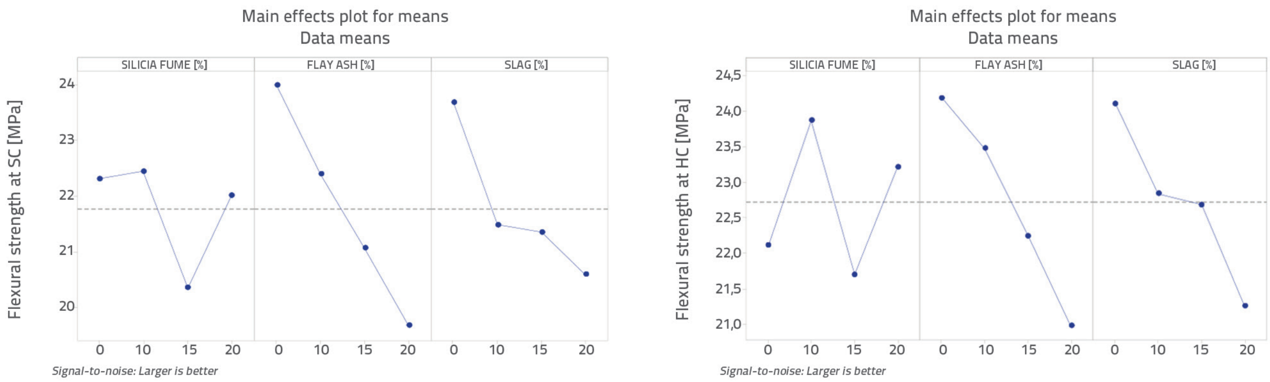

Figure 8. Taguchi optimisation control factor graphs - 2nd part

Table 10. Optimum Taguchi levels and values for strength depending on curing conditions

Test	Control factors	Unit	Optimum level	Optimum value
Compressive strength for SC	SF	%	3	20
	FA	%	1	0
	GBFS	%	1	0
Compressive strength for HC	SF	%	2	10
	FA	%	1	0
	GBFS	%	1	0
Flexural strength for SC	SF	%	2	10
	FA	%	1	0
	GBFS	%	1	0
Flexural strength for HC	SF	%	2	10
	FA	%	1	0
	GBFS	%	1	0

Table 11. Optimal results and validation experiments for control factor 1

Test	Taguchi optimisation	Predicted value			Real value		
		SF	FA	GBFS	SF	FA	GBFS
Compressive strength for SC	Level	3	1	1	3	1	1
	Value	20	0	0	20	0	0
	Result	150.70 MPa			148.37 MPa		
Compressive strength for HC	Level	2	1	1	2	1	1
	Value	10	0	0	10	0	0
	Result	150.43 MPa			147.58 MPa		
Flexural strength for SC	Level	2	1	1	2	1	1
	Value	10	0	0	10	0	0
	Result	26.36 MPa			24.78 MPa		
Flexural strength for HC	Level	2	1	1	2	1	1
	Value	10	0	0	10	0	0
	Result	26.63 MPa			25.98 MPa		

best compressive and flexural strengths are found with group S10F0G0, i.e., 10 % SF, 0 % FA and 0 % GBFS. The results obtained from the verification experiments when controlling the values obtained as a result of the Taguchi optimisation reflect the success of the optimisation. The optimum conditions were estimated and the values obtained as a result of the calculations

Table 12. Optimum Taguchi levels and values for physical properties depending on curing conditions

Test	Control factors	Unit	Optimum level	Optimum value
Water absorption [%]	SF	%	3	15
	FA	%	4	20
	GBFS	%	2	10
Porosity [%]	SF	%	3	15
	FA	%	4	20
	GBFS	%	1	0
Apparent density [kg/m³]	SF	%	1	0
	FA	%	3	15
	GBFS	%	2	10

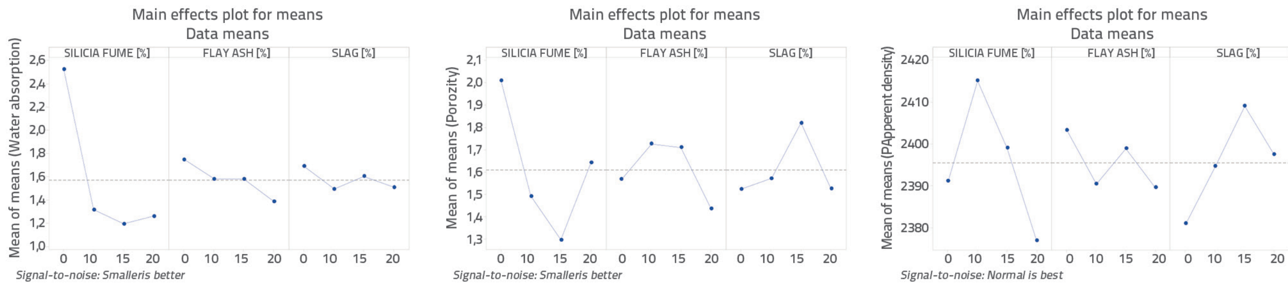

Figure 9. Taguchi optimisation control factor graphs

and those obtained as a result of the verification experiments are presented in Table 11.

3.3.2. Taguchi analysis for physical properties

In terms of the physical properties, the optimum results for the water absorption rate, porosity and apparent density based on the Taguchi L16 experiment matrix are shown in Figure 9. The optimum levels of those results are provided in Table 12.
According to the obtained results, two different mixtures do not fit the L16 group in terms of porosity and apparent density. The water absorption rate and porosity results are the same as those in the S15F20G10 group, i.e.,15 % SF, 20 % FA and 10 % GBFS. The ideal optimum result for the porosity is from the S15F20G0 mixture (15 % SF, 20 % FA and 0 % GBFS), whereas the ideal optimum result for the apparent density is from the S0F15G10 mixture (0 % SF, 15 % FA and 10 % GBFS). The optimum conditions were estimated from the results of the verification experiments performed while controlling the values obtained as a result of the Taguchi optimisation. The values obtained as a result of these calculations and those obtained as a result of the verification experiments are provided in Table 13.

4. Conclusions

The results obtained for UHPCs produced by adding steel fibre, GBFS, FA and SF within the scope of this study are as follows.
The addition of SF results in a reduction in propagation diameter.

Table 13. Optimal results and validation experiments for control factors

Test	Taguchi optimisation	Predicted value			Real value		
		SF	FA	GBFS	SF	FA	GBFS
Water absorption [%]	Level	3	4	2	3	4	2
	Value	15	20	10	15	20	10
	Result	0.93			0.93		
Porosity [%]	Level	3	4	1	3	4	1
	Value	15	20	0	15	20	0
	Result	1.03			1.12		
Apparent density [kg/m³]	Level	1	3	2	2	1	3
	Value	0	15	10	10	0	15
	Result	2393.63			2389		

However, in the case of using FA and GBFS in the mixtures, an increase in the spreading diameter is observed.

Adding SF and FA to UHPC mixtures leads to a decrease in the fresh unit weight, e.g., a decrease from 2339 to 2329 kg/m^{-3} when increasing the amount of SF and from 2347 to 2321 kg/m^{-3} when increasing FA. However, adding GBFS increases the fresh unit volume weight (from 2323 kg/m^{-3} to 2340 kg.m^{-3}).

In the UHPC mixtures, HC leads to higher mechanical strength values compared to those in SC; thus, HC can be used as an acceleration factor to improve the compressive strength. In the HC process, the compressive strength at 28 days is significantly higher than that in the SC samples. In the compressive strength tests, the highest strengths are 147.07 MPa under normal conditions for the S10G10 mixture without FA; in HC conditions, the value is 150.13 MPa.

Increasing the quantities of FA and GBFS decreases the compressive strength of the UHPC in all mixtures. The ratios of the FA and GBFS to the binder added to mixtures of different proportions can be increased by up to 20 % to 35 % in total, but this increase results in decreased early compressive strength of the UHPC. In contrast, adding SF to the mixtures significantly increases the compressive strength. Moreover, the best results for the flexural strengths are similar (26.88 MPa to 27.31 MPa) in both water curing regimes with the S10G10 group, whereas the lowest strengths are obtained from the S15F20G10 group with the GBFS being added to the mixture. Using GBFS, SF and FA in UHPC mixtures to replace the binder may contribute to a decrease in water absorption. The effect of the SF on the porosity may contribute to the production of less-porous materials. The addition of SF and FA to the UHPC mixtures also causes the bulk density to decrease with an increasing ratio of addition, whereas the addition of GBFS causes the density to increase.

Based on the Taguchi analysis of the compression resistance, the impact of the signal-to-noise ratio on the compression resistance was obtained under SC conditions. The maximum compression resistance was obtained from the 20 % SF, 0 % FA and 0 % GBFS mixture. The Taguchi analysis for the flexural strength was obtained in the same water curing and mixture of 10 % SF, 0 % FA and 0 % GBFS. The SF additive was found to be a more useful material to add to UHPCs.

The verification test results values are sufficient for the compressive and flexural strength strengths and physical properties under different curing conditions; thus, Taguchi optimisation can be successfully applied.

Acknowledgements

This study was presented by Ali Alshaab Ramroom as a master's thesis at the Institute of Science, Kastamonu University.

REFERENCES

[1] Najimi, M., Sobhani, J., Ahmadi, B., Shekarchi, M.: An experimental study on durability properties of concrete containing zeolite as a highly reactive natural pozzolan, Constr. Build. Mater., 35 (2012), pp. 1023–1033, https://doi.org/10.1016/j.conbuildmat.2012.04.038.

[2] Eskandari, H., Vaghefi, M., Kowsari, K.: Investigation of Mechanical and Durability Properties of Concrete Influenced by Hybrid Nano Silica and Micro Zeolite, Procedia Mater. Sci., 11 (2015), pp. 594–599, https://doi.org/10.1016/j.mspro.2015.11.084.

[3] Wang, W., Liu, J., Agostini, F., Davy, C.A., Skoczylas, F., Corvez, D.: Durability of an Ultra High Performance Fiber Reinforced Concrete (UHPFRC) under progressive aging, Cem. Concr. Res., 55 (2014), pp. 1–13, https://doi.org/10.1016/j.cemconres.2013.09.008.

[4] Yoo, D.Y., Banthia, N.: Mechanical properties of ultra-high-performance fiber-reinforced concrete: A review, Cem. Concr. Compos., 73 (2016), pp. 267–280, https://doi.org/10.1016/j.cemconcomp.2016.08.001.

[5] Yu, R., Van Beers, L., Spiesz, P., Brouwers, H.J.H.: Impact resistance of a sustainable Ultra-High Performance Fibre Reinforced Concrete (UHPFRC) under pendulum impact loadings, Constr. Build. Mater.,107 (2016), pp. 203–215, https://doi.org/10.1016/j.conbuildmat.2015.12.157.

[6] Memiş, S., Şahin, S., Şirin, Ü.: Some properties of prefabricated building materials produced from ground diatomite and hydrophone clay, Pamukkale Univ. Muh. Bilim. Derg., 23 (2017), pp. 245–249, https://doi.org/10.5505/pajes.2016.34467.

[7] Kaplan, G., Yildizel, S.A., Memiş, S., Öztürk, A.U.: The Optimization of Calcareous Fly Ash-Added Cement Containing Grinding Aids and Strength-Improving Additives, Adv. Civ. Eng., (2018), https://doi.org/10.1155/2018/8917059.

[8] Memis, S., Sahin, S.: Investigation of the effect of press compaction and the use of zeolite on mechanical properties in the production of low strength Reactive Powder Concrete (RPC), Fresenius Environ. Bull., 28 (2019).

[9] Kaplan, G., Yaprak, H., Memiş, S., Alnkaa, A.: Artificial neural network estimation of the effect of varying curing conditions and cement type on hardened concrete properties, Buildings, 9 (2019), https://doi.org/10.3390/buildings9010010.

[10] Liang, X., Wu, C., Yang, Y., Li, Z.: Experimental study on ultra-high performance concrete with high fire resistance under simultaneous effect of elevated temperature and impact loading, Cem. Concr. Compos., 98 (2019), pp. 29–38, https://doi.org/10.1016/j.cemconcomp.2019.01.017.

[11] Yu, R.: Development of sustainable protective ultra-high performance fibre reinforced concrete (UHPFRC): Design, assessment and modeling, Technische Universiteit Eindhoven, 2015.

[12] Meng, W., Valipour, M., Khayat, K.H.: Optimization and performance of cost-effective ultra-high performance concrete, Mater. Struct. Constr., 50 (2017), pp. 1–16, https://doi.org/10.1617/s11527-016-0896-3.

[13] ACI 233R-03: Slag Cement in Concrete and Mortar, Am. Concr. Inst., (2003), pp. 1–19

[14] Liu, Z., El-Tawil, S., Hansen, W., Wang, F.: Effect of slag cement on the properties of ultra-high performance concrete, Constr. Build. Mater., 190 (2018), pp. 830–837, https://doi.org/10.1016/j.conbuildmat.2018.09.173.

[15] Chun, B., Yoo, D.Y.: Hybrid effect of macro and micro steel fibers on the pullout and tensile behaviors of ultra-high-performance concrete, Compos. Part B Eng., 162 (2019), pp. 344–360, https://doi.org/10.1016/j.compositesb.2018.11.026.

[16] Yang, Y., Wu, C., Liu, Z., Liang, X., Xu, S.: Experimental investigation on the dynamic behaviors of UHPFRC after exposure to high temperature, Constr. Build. Mater., 227 (2019), https://doi.org/10.1016/j.conbuildmat.2019.116679.

[17] Zhang, X., Zhao, S., Liu, Z., Wang, F.: Utilization of steel slag in ultra-high performance concrete with enhanced eco-friendliness, Constr. Build. Mater., 214 (2019), pp. 28–36, https://doi.org/10.1016/j.conbuildmat.2019.04.106.

[18] Hou, D., Wu, D., Wang, X., Gao, S., Yu, R., Li, M., Wang, P., Wang, Y.: Sustainable use of red mud in ultra-high performance concrete (UHPC): Design and performance evaluation, Cem. Concr. Compos., 115 (2021), https://doi.org/10.1016/j.cemconcomp.2020.103862.

[19] Moallem, M.R.: Flexural Redistribution in Ultra-High Performance Concrete Lab Specimens, Ohio University, 2010.

[20] Zhang, Y., Cai, S., Zhu, X.,Fan, L. Shao, X.: Flexural responses of steel-UHPC composite beams under hogging moment, Eng. Struct., 206 (2020), https://doi.org/10.1016/j.engstruct.2019.110134.

[21] Alsalman, A., Dang, C.N., Martí-Vargas, J.R., Micah Hale, W.: Mixture-proportioning of economical UHPC mixtures, J. Build. Eng., 27 (2020), https://doi.org/10.1016/j.jobe.2019.100970.

[22] Hung, C.C., Chen, Y.T., Yen, C.H.: Workability, fiber distribution, and mechanical properties of UHPC with hooked end steel macro-fibers, Constr. Build. Mater., 260 (2020), https://doi.org/10.1016/j.conbuildmat.2020.119944.

[23] Memiș, S., Ramroom, A.A.: Investigation of the ideal mixing ratio and steel fiber additive in ultra high performance concrete, Rev. Rom. Mater. Rom. J. Mater., 50 (2020), pp. 403–410

[24] Shen, P., Zheng, H., Xuan, D., Lu, J.X., Poon, C.S.: Feasible use of municipal solid waste incineration bottom ash in ultra-high performance concrete, Cem. Concr. Compos., 114 (2020), https://doi.org/10.1016/j.cemconcomp.2020.103814.

[25] TS EN 197-1: Cement--Part 1: Compositions and conformity criteria for common cements, Turkish Stand. Inst., 2002.

[26] ASTM C 1240: Standard Specification for Silica Fume Used in Cementitious Mixtures, American society for testing and materials, 2 (2020).

[27] ASTM C618: Standard specification for coal fly ash and raw or calcined natural pozzolan for use in concrete, American society for testing and materials, 2003.

[28] ASTM C33 / C33M – 18: Standard Specification for Concrete Aggregates, ASTM Int., 2018.

[29] ASTM C 136 / C136M-19, Standard Test Method for Sieve Analysis of Fine and Coarse Aggregates, ASTM Int., 2014.

[30] Hirata, T., Ye, Z., Branicio, J.P., Zheng, J., Lange, A., Plank, J., Sullivan, M.: Adsorbed Conformations of PCE Superplasticizers in Cement Pore Solution Unraveled by Molecular Dynamics Simulations, Sci. Rep., 7 (2017), https://doi.org/10.1038/s41598-017-16048-3

[31] Roy, R.K.: A Primer on the Taguchi Method, Society of Manufacturing Engineers, 1990.

[32] Nuruddin, M., Bayuaji, R.: Application of Taguchi's approach in the optimization of mix proportion for Microwave Incinerated Rice Husk Ash foamed concrete, IJCEE, 9 (2009), pp. 121–129

[33] Nuruddin, M.F.B., Bayuji, R.: Optimum Mix Proportioning of Mirha Foamed Concrete Using Taguchi's Approach, Apsec-Eacef, (2009), pp. 694–700

[34] Türkmen, I., Gül, R., Çelik, C.: A Taguchi approach for investigation of some physical properties of concrete produced from mineral admixtures, Build. Environ., 43 (2008), pp. 1127–1137, https://doi.org/10.1016/j.buildenv.2007.02.005

[35] Torregrosa, E.C.: Dosage optimization and bolted connections for UHPFRC ties, Master Thesis, Riunet, 2013., pp. 1–276

[36] Fehling, E., Schmidt, M., Stürwald, S.: Ultra High Performance Concrete (UHPC), Proceedings of the Second International Symposium on Ultra High Performance Concrete, Kassel, Germany, 2008.

[37] Wang, D., Shi, C., Wu, Z., Xiao, J., Huang, Z., Fang, Z.: A review on ultra high performance concrete: Part II - Hydration, microstructure and properties, Constr. Build. Mater., 96 (2015), pp. 368–377, https://doi.org/10.1016/j.conbuildmat.2015.08.095.

[38] Christ, R., Pacheco, F., Ehrenbring, H., Quinino, U., Mancio, M., Muñoz, Y. Tutikian, B.: Study of mechanical behavior of ultra - High performance concrete (UHPC) reinforced with hybrid fibers and with reduced cement consumption, Rev. Ing. Constr., 34 (2019), pp. 159–168, https://doi.org/10.4067/S0718-50732019000200159.

[39] Toutlemonde, F., Resplendino, J.: Designing and Building with UHPFRC, Wiley, 2013., https://doi.org/10.1002/9781118557839.

[40] Li, P.P., Yu, Q.L., Brouwers, H.J.H.: Effect of PCE-type superplasticizer on early-age behaviour of ultra-high performance concrete (UHPC), Constr. Build. Mater., 153 (2017), pp. 740–750, https://doi.org/10.1016/j.conbuildmat.2017.07.145.

[41] Wang, C., Yang, C., Liu, F., Wan, C., Pu, X.: Preparation of Ultra-High Performance Concrete with common technology and materials, Cem. Concr. Compos., 34 (2012), pp. 538–544, https://doi.org/10.1016/j.cemconcomp.2011.11.005.

[42] Shi, C., Mo, Y.L.: High-performance Construction Materials: Science and Applications, World Scientific, 2008.

[43] Chu, S.H., Kwan, A.K.H.: Mixture design of self-levelling ultra-high performance FRC, Constr. Build. Mater., 228 (2019), https://doi.org/10.1016/j.conbuildmat.2019.116761.

[44] Prem, P.R., Bharatkumar, B.H., Iyer, N.R.: Influence of curing regimes on compressive strength of ultra high performance concrete, Sadhana - Acad. Proc. Eng. Sci., 38 (2013), pp. 1421–1431, https://doi.org/10.1007/s12046-013-0159-8.

[45] ASTM C192 / C192M-19: Standard Practice for Making and Curing Concrete Test Specimens in the Laboratory, ASTM Int., 2019.

[46] ASTM C1437-20: Standard Test Method for Flow of Hydraulic Cement Mortar, ASTM Int., 2020.

[47] ASTM C138 / C138M-17a: Standard Test Method for Density (Unit Weight), Yield and Air Content (Gravimetric) of Concrete, ASTM Int., 2017.

[48] BS EN 196-1: British Standard Methods of testing cement, 3 (2005).

[49] ASTM C642: Standard Test Method for Density, Absorption and Voids in Hardened Concrete 1, 1997., pp. 1–3.

[50] Lamond, J.F., Pielert, J.H.: Significance of Tests and Properties of Concrete and Concrete-Making STP 169D, 2006.

[51] ACI 234R-06, 234R-06: Guide for the Use of Silica Fume in Concrete, Aci 234R-06, 96 (2006), pp. 1–64

[52] Schmidt, M., Fehling, E., Glotzbach, C., Fröhlich, S., Piotrowski, S.: Heft 19 Schriftenreihe Baustoffe und Massivbau Ultra-High Performance Concrete and Nanotechnology, 2012.

[53] Bajaber, M.A., Hakeem, I.Y.: UHPC evolution, development, and utilization in construction: A review, J. Mater. Res. Technol., 10 (2021), pp. 1058–1074, https://doi.org/10.1016/j.jmrt.2020.12.051

[54] Xincheng, P.: Super-High-Strength High Performance Concrete, Taylor & Francis, 2012.

[55] Zulu, S.N.F.: Optimizing the usage of fly ash in concrete mixes, Durban University of Technology, 2017.

[56] Hiremath, P., Yaragal, S.C.: Investigation on Mechanical Properties of Reactive Powder Concrete under Different Curing Regimes, Mater. Today, 4 (2017), pp. 9758–9762, https://doi.org/10.1016/j.matpr.2017.06.262.

[57] Maltais, Y., Marchand, J.: Influence of curing temperature on cement hydration and mechanical strength development of fly ash mortars, Cem. Concr. Res., 27 (1997), pp. 1009–1020, https://doi.org/10.1016/S0008-8846(97)00098-7.

[58] Gonen, T., Yazicioglu, S.: The influence of mineral admixtures on the short and long-term performance of concrete, Build. Environ., 42 (2007), pp. 3080–3085, https://doi.org/10.1016/j.buildenv.2006.10.019

[59] Wang, A., Zhang, C., Sun, W.: Fly ash effects: II. The active effect of fly ash, Cem. Concr. Res., 34 (2004), pp. 2057–2060, https://doi.org/10.1016/j.cemconres.2003.03.001.

[60] Kumar, S.: Fly ash-lime-phosphogympsum hollow blocks for walls and partitions, Build. Environ., 38 (2003), pp. 291–295, https://doi.org/10.1016/S0360-1323(02)00068-9.